Environmental Pollution 263 (2020) 114593

Contents lists available at ScienceDirect

Environmental Pollution

journal homepage: www.elsevier.com/locate/envpol

The influence of nanoplastics on the toxic effects, bioaccumulation, biodegradation and enantioselectivity of ibuprofen in freshwater algae *Chlorella pyrenoidosa*☆

Fang Wang [a], Bin Wang [a, b, *], Han Qu [a, c], Wenxing Zhao [a], Lei Duan [a], Yizhe Zhang [a], Yitong Zhou [a], Gang Yu [a, b]

[a] School of Environment, Beijing Key Laboratory for Emerging Organic Contaminants Control, State Key Joint Laboratory of Environment Simulation and Pollution Control (SKLESPC), Tsinghua University, Beijing, 100084, PR China
[b] Research Institute for Environmental Innovation (Suzhou), Tsinghua, Building 16, 101 Business Park, No, 158 Jinfeng Road, New District, Suzhou, 215163, China
[c] Department of Pharmacology, College of Medicine, The University of Arizona, Tucson, AZ, 85712, United States

ARTICLE INFO

Article history:
Received 30 January 2020
Received in revised form
25 March 2020
Accepted 11 April 2020
Available online 15 April 2020

Keywords:
Nanoplastics
PPCPs
Aquatic pollution
Combined pollution
Combined effects

ABSTRACT

Plastic pollution has become a pressing issue due to its persistence in the environment. Smaller plastics are more easily ingested, potentially exerting greater influences on organisms. In this study, the effects of polystyrene nanoplastics (NP) on the toxic effects, bioaccumulation, biodegradation and enantioselectivity of ibuprofen (IBU) in algae *Chlorella pyrenoidosa* were explored. The influences on the growth rate, chlorophyll *a*, total antioxidant capacity (T-AOC), reactive oxygen species (ROS) and lipid peroxidation (MDA) were evaluated after 96 h of exposure to a combination of polystryene NP (1 mg L^{-1}) and IBU (5−100 mg L^{-1}). The results indicated that the inhibitory effect of IBU on *C. pyrenoidosa* growth was alleviated in the presence of NP. For instance, the 96 h-IC_{50} value for rac-IBU in the treatment lacking NP was 45.7 mg L^{-1}, and the corresponding value in the treatment containing NP was 63.9 mg L^{-1}. The co-exposure of NP led to a significant enhancement of T-AOC and slight reduction of ROS and MDA compared with the individual exposure (IBU) group, suggesting a decreased oxidative stress. In addition, treatment with NP led to a decreased bioaccumulation and accelerated biodegradation of IBU in *C. pyrenoidosa* and enhanced removal in the medium. The enantioselective toxicity, bioaccumulation and biodegradation of IBU were observed both in the absence and presence of NP. S-IBU exhibited a greater toxicity, and R-IBU was preferentially accumulated and degraded in *C. pyrenoidosa*. No interconversion of the two enantiomers occurred regardless of the presence of NP. This consequence implied that the influence of coexistent NP should be considered in the environmental risk assessment of pharmaceuticals and personal care products in aquatic environments.

1. Introduction

Plastics have been widely used in various fields, including industry, agriculture, medicine and packing, since they were invented. Because of the large amount of production and difficulty in degradation, many plastics are released into the environment. Plastics are quite persistent in the environment due to their chemical inertness; however, their size could decrease under the effects of wind waves and tides. Currently, microplastics (plastics smaller than 5 mm) are widespread in oceans and freshwater ecosystems (Eriksen et al., 2014; Jambeck et al., 2015; Thompson et al., 2004). For instance, the abundance of microplastics is as high as 1.4×10^7 particles·km^{-2} in the main stream of the Yangtze River in Yichang and 3.9×10^6 particles·km^{-2} in the surface of the Rhine River between Basel and Rotterdam (Mani et al., 2015; Zhang et al., 2015a). Previous studies have indicated that microplastics may exert several negative effects on organisms. For instance, microplastics could reduce the energy intake and impact the fecundity and offspring performance of aquatic organisms

☆ This paper has been recommended for acceptance by Maria Cristina Fossi.

* Corresponding author. School of Environment, Tsinghua University, Beijing, 100084, PR China.
E-mail address: thuwb@tsinghua.edu.cn (B. Wang).

https://doi.org/10.1016/j.envpol.2020.114593
0269-7491/

(Sussarellu et al., 2016). However, recent studies have discovered the potential for fragmentation of plastic polymers into nanoplastics (NP), which may exhibit remarkably different properties from the bulk polymer due to their small sizes (Lambert and Wagner, 2016). In addition, the influence of NP contamination on the environmental behavior of other co-existing pollutants still needs further investigation.

Pharmaceuticals and personal care products (PPCPs) play an irreplaceable role in human life. Unfortunately, PPCPs have been detected in surface and drinking water due to their high production amount and insufficient removal in wastewater treatment plants, which has become a growing concern (Kasprzyk-Hordern et al., 2009; Loraine and Pettigrove, 2006). Ibuprofen (IBU) is a non-steroidal anti-inflammatory drug that is extensively used for the alleviation of pain, inflammation and fever. IBU has been detected in most wastewater and surface water samples, with maximum reported concentration levels of 373 μg L^{-1} and 1417 ng L^{-1}, respectively (Peng et al., 2008; Santos et al., 2007). On account of its high detection frequency, occurrence level and relatively high toxicity in aquatic environments, IBU has been identified as a priority PPCP that poses greater potential risks (Bu et al., 2013).

IBU consists of two enantiomers that may exhibit different activities, toxicities and degradation behaviors in the environment (Baird et al., 2013; Ye et al., 2013; Zhang et al., 2015b). For instance, S-fluoxetine, which is used for migraine prophylaxis, is more toxic to *Pimephales promelas* than R-fluoxetine, which is an antidepressant (Stanley et al., 2007; Steiner et al., 1998). The more active enantiomer S-amphetamine degrades faster than R-amphetamine in river and urban waters (Bagnall et al., 2013; Evans et al., 2016; Kasprzyk-Hordern et al., 2010). Previous research has indicated that IBU induces enantioselective metabolic disorders in zebrafish (Song et al., 2018). Pharmacologically active S-IBU is preferentially degraded in lake water and wastewater, and can transform into R-IBU during wastewater treatment processes (Buser et al., 1999; Khan et al., 2014; Matamoros et al., 2009). Pharmacologically inactive R-IBU is preferentially degraded in river water and activated sludge and can convert into S-IBU during human metabolism (Escuder-Gilabert et al., 2018; Hao et al., 2005; Winkler et al., 2001). However, the enantioselective accumulation, degradation and chiral transformation of IBU in aquatic organisms are poorly documented.

As an important producer in aquatic systems, algae plays a crucial role in generating oxygen and providing food for higher trophic levels, potentially maintaining the stability of ecosystems. *Chlorella pyrenoidosa (C. pyrenoidosa)* is a freshwater unicellular green algae that is sensitive to pollutants in aquatic environments and is commonly regarded as a model organism in ecotoxicity tests (Xia et al., 2018; Zhang et al., 2016a; Zhao et al., 2017). In addition, *C. pyrenoidosa* is capable of accumulating and removing pollutants in aquatic environments, such as pesticides, antimicrobial agents and steroid hormones (Gao et al., 2019; Peng et al., 2014; Wang et al., 2018).

Therefore, this study aimed to determine if NP had an effect on the toxic effects, bioaccumulation, biodegradation, and enantioselectivity of IBU in freshwater green algae *C. pyrenoidosa*. The IBU concentration inducing 50% growth rate inhibition (IC_{50}) was obtained, and the changes in chlorophyll *a*, total antioxidant capacity (T-AOC), reactive oxygen species (ROS) and lipid peroxidation (MDA) in *C. pyrenoidosa* were monitored in the absence and presence of NP. Racemate treatment was conducted to examine the effects of NP on the bioaccumulation and biodegradation of IBU in *C. pyrenoidosa*. Individual enantiomer treatments were carried out to investigate the effects of NP on the enantioselectivity and chiral interconversion of IBU. The concentrations of IBU were detected both in the medium and in *C. pyrenoidosa*. This work could be helpful for understanding the environmental risks of NP.

2. Materials and methods

2.1. Chemicals and reagents

Racemic- (rac-), R- and S-IBU (purity all above 98%, Aladdin) were dissolved in acetone to obtain stock solutions. Red fluorescently labeled polystyrene (PS) NP (600 nm, 620/680 nm excitation/emission, water 1:1 emulsion, 1% w/v) was bought from Tianjin BaseLine Chromatography Technology Research Center (Tianjin, China). Working solutions of IBU and NP were prepared by diluting stock solutions with acetone and ultrapure water, respectively, prior to use. BG11 medium was purchased from Qingdao Hope bio-Technology Co., Ltd. (Qingdao, China) and autoclaved at 121 °C for 30 min. All reagents from Avantor Performance Materials (Center Valley, PA) were of chromatographic grade, and the water was purified by a Milli-Q system.

2.2. Algae cultivation

Algae *C. pyrenoidosa* were obtained from the Institute of Hydrobiology, the Chinese Academy of Science. They were cultured in the BG11 medium at 25±1 °C under the illumination of 70 μmol photons·m^{-2} s^{-1} with a 12/12 light/dark cycle.

2.3. Characterization of NP in the medium

NP were suspended at 1 mg L^{-1} in the control BG11 medium without algae. The effective diameter and zeta potential of the NP were measured after 0, 24, 48 and 96 h of preparation using a Nanobrook Omni analyzer (Nano-brook Omni, Brookhaven, US). The effective diameter was determined by dynamic light scattering (DLS) measurements, and the zeta potential was analyzed by phase analysis light scattering (PALS) measurements.

2.4. Growth inhibition test

The test was conducted based on OECD guideline 201 (OECD, 2011). All glassware used were cleaned and sterilized. Algae in the exponential phase were inoculated into 250-mL flasks filled with 100 mL of exposure medium at a density of 2.5×10^5 cells·mL^{-1}. The exposure concentrations of rac-/R-/S- IBU ranged from 5 to 100 mg L^{-1} (5, 25, 50, 75 and 100 mg L^{-1}), and all treatments for each chemical tested were performed with (co-exposure) and without 1 mg L^{-1} NP (individual exposure). Control (acetone) and NP treatment (1 mg L^{-1} NP) were also undertaken, and the volume of solvents was below 0.1% V/V. The test was triplicated under the same conditions as cultivation. The flasks were manually shaken three times and randomly replaced in the incubator every day. After exposure for 48, 72 and 96 h, the algae density was determined by measuring the optical density of the suspension at a wavelength of 650 nm. The average growth rate and percentage of growth inhibition were calculated. The IC_{50} (the inhibitory concentration that results in a 50% reduction in the algae growth rate compared to the control) was determined by plotting the inhibition percentage against the logarithm of the concentration.

The effect of NP shading on algae growth was investigated. In brief, a 250-mL flask filled with 100 mL of the algae suspension was transferred into a 1-L beaker containing 1 mg L^{-1} NP in the algae suspension. The group with the NP-free algae suspension in the beaker served as the control. The liquid level of the suspension in the beaker was adjusted to maintain the same height as that in the flask. The algae cell density in the flask was measured after 96 h of

exposure, and the inhibition effect of NP shading on algae growth was calculated.

2.5. Physiological and biochemical tests

After exposure for 96 h, the chlorophyll, ROS, protein, T-AOC and MDA of the algae were monitored. (1) The chlorophyll *a* content was determined by measuring the chlorophyll *a* fluorescence. One milliliter of the suspension was sampled and centrifuged at 1500 g min^{-1} for 10 min at 4 °C. The algae residues were extracted with 1 mL of a 90% (V/V) acetone aqueous solution, followed by ultrasonic treatment for 20 min in an ice bath. The residues were then placed in the dark for 24 h. The fluorescence intensity of the supernatant was recorded at an excitation of 430 nm and an emission of 670 nm. (2) The intracellular ROS production was measured using the fluorescent probe 2′,7′-dichlorofluorescin diacetate (DCFH-DA). A certain volume of the suspension containing one million algae cells was collected and centrifuged at 1500 g min^{-1} for 10 min at 4 °C. After being washed with a 0.1 M phosphate buffered saline (PBS) solution (pH = 7) three times, the algae residues were incubated with 10 μM DCFH-DA for 60 min at 37 °C in the dark. At the end of the incubation, the working DCFH-DA was removed, and the algae cells were washed twice with the 0.1 M PBS solution (pH = 7) and resuspended in 200 μL of PBS. The fluorescence intensity was determined at excitation and emission wavelengths of 500 nm and 520 nm, respectively. (3) Approximately 40 mL of the suspension was centrifuged at 1500 g min^{-1} for 10 min at 4 °C. The algae residues were suspended in 3 mL of the 0.1 M PBS solution (pH = 7) and subjected to cycles of 5 s of sonication and 5 s of pause during ultrasonic treatment at 200 W over a period of 5 min. After centrifugation at 13700*g* for 10 min at 4 °C, the supernatant was used to evaluate the protein, T-AOC and MDA. The protein level was determined based on the Coomassie Brilliant Blue G250 (Bradford, 1976). The T-AOC level was assessed based on the method of 3-ethylbenzthiazoline-6-sulfonic acid (ABTS) (Re et al., 1999). Antioxidants inhibit the conversion of ABTS to $ABTS^{+}$, and the T-AOC was determined by monitoring the decrease of $ABTS^{+}$ at 405 nm. Trolox was used as a reference standard, and the results were expressed as moles of Trolox per mass of protein. MDA was assayed by monitoring the appearance of MDA-thiobarbituric acid (TBA) adduct at 532 nm (Heath and Packer, 1968).

2.6. Accumulation and degradation tests

Sterilized flasks filled with 100 mL of exposure medium were inoculated with pre-cultured algae in the exponential growth phase at a density of 2.5 × 10^5 cells·mL^{-1}. The exposure concentrations of rac-/R-/S- IBU were set at 0.5 mg L^{-1}, and all chemicals tested were performed with and without 1 mg L^{-1} NP. The group with the algae-free suspension served as the control to explore the abiotic degradation of IBU. The volume of solvents was under 0.1% v/v, and the experiments were performed in triplicate under the same cultivation conditions. The flasks were shaken manually three times, and their position in the incubator was randomly changed every day. Approximately 5 mL of the algae suspension was sampled at day 2, 3, 5, 7, 10, 14, 21, 28, 35 and 42.

2.7. Sample extraction

The suspension was centrifuged at 1500 g min^{-1} for 10 min at 4 °C, and the supernatant medium and *C. pyrenoidosa* were extracted separately. After the addition of 100 μL of 1 M HCl, the supernatant medium was extracted twice with 4 mL of an n-hexane/ethyl acetate (4:1) mixture. The mixtures were vortex-mixed for 3 min and centrifuged at 9500 *g* for 10 min. The algae residue was extracted twice with 4 mL of the n-hexane/methane (1:2) mixture, followed by ultrasonic treatment for 1 h. The residues were then subjected to centrifugation at 9500*g* for 10 min. The organic phase was combined and dried under gentle nitrogen flow. The residues were redissolved in 0.5 mL of acetonitrile and passed through a 0.22 μm filtration membrane prior to analysis.

2.8. Analytical methods

The concentrations of IBU were monitored using an UHPLC Ultimate 3000 system in combination with a triple quadrupole mass spectrometer API 3200 (AB Sciex, USA). Detection was performed in negative ion multiple reaction monitoring (MRM) mode. The following conditions were used: ionspray voltage −4500 V; source temperature 500 °C; curtain gas 20 psi; collision gas 5 psi; nebulizer gas 40 psi; turbo gas 60 psi; entrance potential −10 V; declustering potential −23 V; collision energy −16 V; and collision cell exit potential −2 V. The parent/product ion pair at m/z 205.1 and 161.1 was chosen for quantification. R-and S-IBU were separated on a Chiralpal AD-RH (150 × 4.6 mm, 5 μm, Daicel Chemical Industries Ltd, Japan) column maintained at 25 °C. The mobile phase consisted of acetonitrile/10 mM ammonium acetate (4/6, pH = 5) with a flow rate of 0.5 mL min^{-1}. The retention times of R- and S-IBU were 12.0 and 13.0 min, respectively.

2.9. Method validation

The recovery experiment was conducted by spiking rac-IBU into the blank medium and the algae residues at three different doses. The limit of detection (LOD) and the limit of quantification (LOQ) were estimated on the basis of signal-to-noise ratios (S/N) of 3 and 10, respectively. Linear curves were obtained by plotting the peak areas versus the concentrations over the range of 0.01–1 mg L^{-1} in the medium and 0.1–10 mg kg^{-1} in the algae. The precision of the method was explored by three replicates.

2.10. Data analysis

Statistical analysis was carried out using SPSS 21.0 and all data represented the means of three replicates. One-way analysis of variance (ANOVA) was conducted to identify significant differences between individual exposure (IBU) and co-exposure (IBU + NP) groups.

The degradation of pollutants usually followed first-order reaction kinetics. The degradation rate constant *k* and the half-life $T_{1/2}$ were determined by the following equations:

$$C_t = C_0 e^{-kt}$$

$$T_{1/2} = \ln 2 \Big/ k$$

where C_t is the concentration at time t (day); C_0 is the initial concentration; *k* is the degradation rate constant; t is the exposure time (day); and $T_{1/2}$ is the degradation half-life.

The enantiomeric fraction (EF) value was determined by the following equation to investigate the enantioselective accumulation and metabolism of IBU in the medium and in *C. pyrenoidosa*.

$$EF = \frac{C_R}{C_R + C_S}$$

where C_R and C_S are the concentrations of R-IBU and S-IBU,

respectively.

3. Results

3.1. Method validation

The recoveries of IBU ranged from 76% to 93% in the medium and from 88% to 94% in *C. pyrenoidosa,* with RSD values below 12%. Good linear relationships between the peak areas and the concentrations were obtained over the range of 0.01–1 mg L^{-1} in the medium and 0.1–10 mg kg^{-1} in *C. pyrenoidosa,* with a correlation coefficient (R^2) greater than 0.995. The LOQs were determined at 1.1 μg L^{-1} in the medium and 3.6 μg kg^{-1} in *C. pyrenoidosa*, and the LODs were found to be 0.3 μg L^{-1} in the medium and 1.1 μg kg^{-1} in *C. pyrenoidosa.*

3.2. Characterization of NP in the medium

As displayed in Fig. S1A, the effective diameter remained at the same level over the 96 h period, suggesting that no agglomeration of NP occurred in the control medium. The absolute zeta potential values (Fig. S1B) first increased and stayed relatively constant until the end of the measurement, indicating that the NP reached a stable state in the control medium after 2 days.

3.3. Growth inhibition test

Table 1 summarizes the IC_{50} values for rac-, R- and S-IBU in the absence and presence of 1 mg L^{-1} NP. As the exposure time increased, the IC_{50} value exhibited a decreasing trend, suggesting that the inhibitory effect increased as the exposure time increased. For instance, the IC_{50} value for rac-IBU decreased from 64.1 to 48.5 mg L^{-1} when the exposure duration increased from 48 h to 96 h. In the treatments without NP, the enantioselective toxicity was observed with S-IBU (96 h-IC_{50} = 54.5 mg L^{-1}) being more toxic to *C. pyrenoidosa* than R-IBU (96 h-IC_{50} = 61.0 mg L^{-1}).

The treatment with 1 mg L^{-1} NP alone led to inhibition impacts on the growth of *C. pyrenoidosa*, with a growth inhibition of 15.6 ± 3.5% compared with the control group after 4 days of exposure. However, when medium was contaminated with NP, the IC_{50} values for rac-, R- and S-IBU increased compared with the individual exposure group. For example, the 96 h-IC_{50} value for rac-IBU in the NP-free treatment was 48.5 mg L^{-1}, and the corresponding value in the treatment containing NP was 67.9 mg L^{-1}. This suggested that NP alleviated the inhibitory effect of IBU on *C. pyrenoidosa* growth. The IC_{50} value of R-IBU (96 h-IC_{50} = 63.4 mg L^{-1}) was greater than that of S-IBU (96 h-IC_{50} = 55.0 mg L^{-1}), indicating that the enantioselective toxicity remained in the treatments containing NP. Then, the physiological and biochemical tests were carried out to investigate the possible reason for the decreased toxicity of IBU.

3.4. Physiological and biochemical tests

Based on the results of the growth inhibition test, *C. pyrenoidosa* samples exposed to three doses 5, 50 and 100 mg L^{-1} of IBU (IC_{10}, IC_{50}, IC_{90}) were collected after 4 days of exposure to investigate the physiological and biochemical responses.

Fig. 1 shows the chlorophyll fluorescence (Fig. 1A), T-AOC (Fig. 1B), ROS (Fig. 1C) and MDA (Fig. 1D) of *C. pyrenoidosa* as a function of the rac-IBU concentration in the absence of NP. The chlorophyll fluorescence declined as the concentration increased, whereas T-AOC, ROS and MDA exhibited an increasing trend as the concentration increased. Chlorophyll fluorescence, T-AOC, ROS and MDA were not significantly affected when exposed to rac-IBU at the lowest concentration (5 mg L^{-1}) compared with the control group; however, they were obviously influenced when the concentration increased to 50 mg L^{-1} and 100 mg L^{-1}.

The individual treatment with 1 mg L^{-1} NP showed no apparent impacts on the chlorophyll fluorescence, T-AOC, ROS and MDA of *C. pyrenoidosa* in comparison with the control group (Fig. 1). However, the co-exposure of rac-IBU with NP produced an elevation in the T-AOC (Fig. 1B), ROS (Fig. 1C) and MDA (Fig. 1D), and caused a reduction in the chlorophyll fluorescence (Fig. 1A). When compared with the individual exposure (rac-IBU) group, the T-AOC significantly enhanced while the ROS and MDA slightly decreased, suggesting co-exposure of NP led to a decreased oxidative stress.

To determine if co-exposure of NP influences the enantioselective oxidative stress of IBU, R- and S-IBU exposure groups were examined. As seen from Fig. 2, the chlorophyll fluorescence (Fig. 2A), T-AOC (Fig. 2B), ROS (Fig. 2C) and MDA (Fig. 2D) exhibited similar trends upon exposure to R- and S-IBU in the treatment without NP. As the concentration increased, the chlorophyll fluorescence showed a decreasing trend, and the T-AOC, ROS and MDA increased as the exposure time increased. No significant differences in chlorophyll fluorescence between the R- and S-IBU exposure groups were observed at any dose of IBU. However, S-IBU caused slightly more ROS and a significant enhancement in the T-AOC and MDA compared to R-IBU, indicating S-IBU could induced greater oxidative stress than R-IBU.

The co-exposure to NP increased the levels of fluorescence and T-AOC, and decreased the ROS and MDA induced by R-IBU or S-IBU (Fig. S3 and Fig. S4), which was consistent with the results of rac-IBU. As shown in Fig. 3, there were also significant differences in the T-AOC (Fig. 3B) and MDA (Fig. 3D) between and the R- and S-IBU treatments in the presence of NP, with the co-exposure of S-IBU with NP inducing greater oxidative stress. These results showed that the co-presence of 1 mg L^{-1} NP had no effect on the enantioselective oxidative stress of IBU on *C. pyrenoidosa*.

3.5. Bioaccumulation and biodegradation of IBU in C. pyrenoidosa

Fig. 4A shows the concentrations-time curves of rac-IBU in *C. pyrenoidosa*. In the treatments lacking NP, the concentration of rac-IBU increased to 3.3 mg kg^{-1} on the third day then

Table 1
Calculated IC_{50} values of rac-, R- and S-IBU in the absence and presence of 1 mg L^{-1} NP.

	48 h		72 h		96 h	
	IC_{50} (mg·L^{-1})	R^2	IC_{50} (mg·L^{-1})	R^2	IC_{50} (mg·L^{-1})	R^2
rac-IBU	64.1	0.931	52.8	0.904	48.5	0.926
R-IBU	66.7	0.981	64.4	0.938	61.0	0.984
S-IBU	65.5	0.926	53.8	0.960	54.5	0.974
rac-IBU + NP	>100	–	66.5	0.982	67.9	0.978
R-IBU + NP	>100	–	68.5	0.831	63.4	0.956
S-IBU + NP	95.7	0.839	57.4	0.927	55.0	0.855

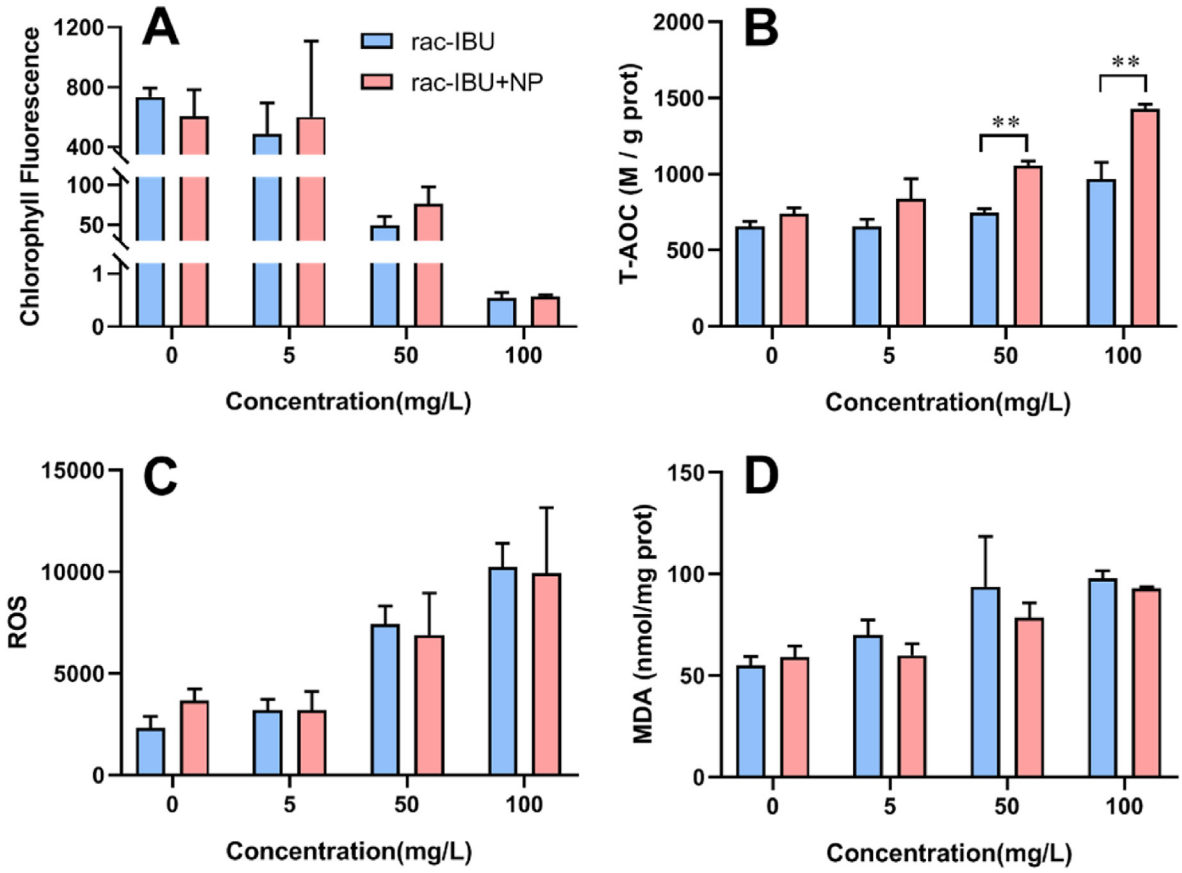

Fig. 1. The influences on (A) chlorophyll fluorescence, (B) T-AOC, (C) ROS and (D) MDA of *C. pyrenoidosa* exposed to rac-IBU in the absence and presence of 1 mg L^{-1} NP. The results are the means from three independent replicates; the error bars correspond to the standard deviation; one and two asterisks denote significant differences between individual exposure (rac-IBU) and co-exposure (rac-IBU + NP) groups at $p < 0.05$ and $p < 0.01$, respectively (LSD Test).

progressively decreased to 1.1 mg kg^{-1} on the last day of treatment. The degradation of rac-IBU in *C. pyrenoidosa* showed a half-life of 28.9 days (Table 2). Slight differences in the concentrations of R- and S-IBU were observed. The EF value of IBU in *C. pyrenoidosa* (Fig. 5A) increased from 0.5 to 0.58 after three days, which may be attributed to the preferential accumulation of R-IBU or interconversion between enantiomers. After that, the EF value progressively decreased to 0.52 at the end of the experiment, which was probably caused by the preferential degradation of R-IBU or interconversion between enantiomers.

In the treatments containing NP, the concentration of rac-IBU increased to 2.8 mg kg^{-1} after three days, and then gradually decreased to 0.8 mg kg^{-1} at the end of the experiment. The calculated half-life of rac-IBU in *C. pyrenoidosa* was 24.8 days in the presence of NP. The EF value of IBU increased from 0.5 to 0.57 over the first three days and then progressively declined to 0.52 on the last day of exposure, which may be due to the preferential accumulation and degradation of R-IBU or interconversion between enantiomers. The accumulated maximum concentrations and half-life values in the co-exposure treatment (rac-IBU + NP) were lower than those of the individual exposure (rac-IBU) treatment, suggesting that the co-presence of 1 mg L^{-1} NP could slightly reduce the accumulation amount and the degradation half-life of rac-IBU in *C. pyrenoidosa*.

Individual R- and S-IBU exposure experiments were also performed to further investigate whether or not NP had an effect on the enantioselective accumulation, degradation and chiral inversion of IBU. In the treatment without NP, as shown in Fig. 4B, the levels of R- and S-IBU peaked on the third day and gradually decreased after that. Enantioselective accumulation and degradation of IBU were found, with R-IBU being preferentially accumulated and degraded in *C. pyrenoidosa*. The maximum accumulation amount of R-IBU was slightly higher than that of S-IBU and the degradation of R-IBU in *C. pyrenoidosa* was slightly faster than that of S-IBU, with half-lives of 22.4 and 23.9 days, respectively. No interconversion of the two enantiomers was observed. In the treatments containing NP, as shown in Fig. 4C, the concentrations of R- and S-IBU reached the maximum level on the third day and gradually declined after that. Similarly, preferential accumulation and degradation of R-IBU were found. The concentration of R-IBU was slightly higher than that of S-IBU in the accumulation stage and the half-lives of R- and S-IBU were 19.8 and 23.1 days, respectively, in *C. pyrenoidosa* in the presence of NP. No interconversion of the two enantiomers was found. Based on Fig. 4B and C, the co-presence of 1 mg L^{-1} NP had no effect on the enantioselective accumulation and degradation of IBU in *C. pyrenoidosa*.

3.6. Removal of IBU in the medium

The abiotic degradation of IBU throughout the experiment was examined in the control medium without algae. Considering that enantiomers have identical abiotic degradation rates, the experiment was conducted with rac-IBU. As shown in Fig. S2, the abiotic degradation of rac-IBU was quite slow in the control medium with a half-life above 42 days. In the NP-free medium, the degradation rate of rac-IBU was 25.9% on the last day, and the corresponding

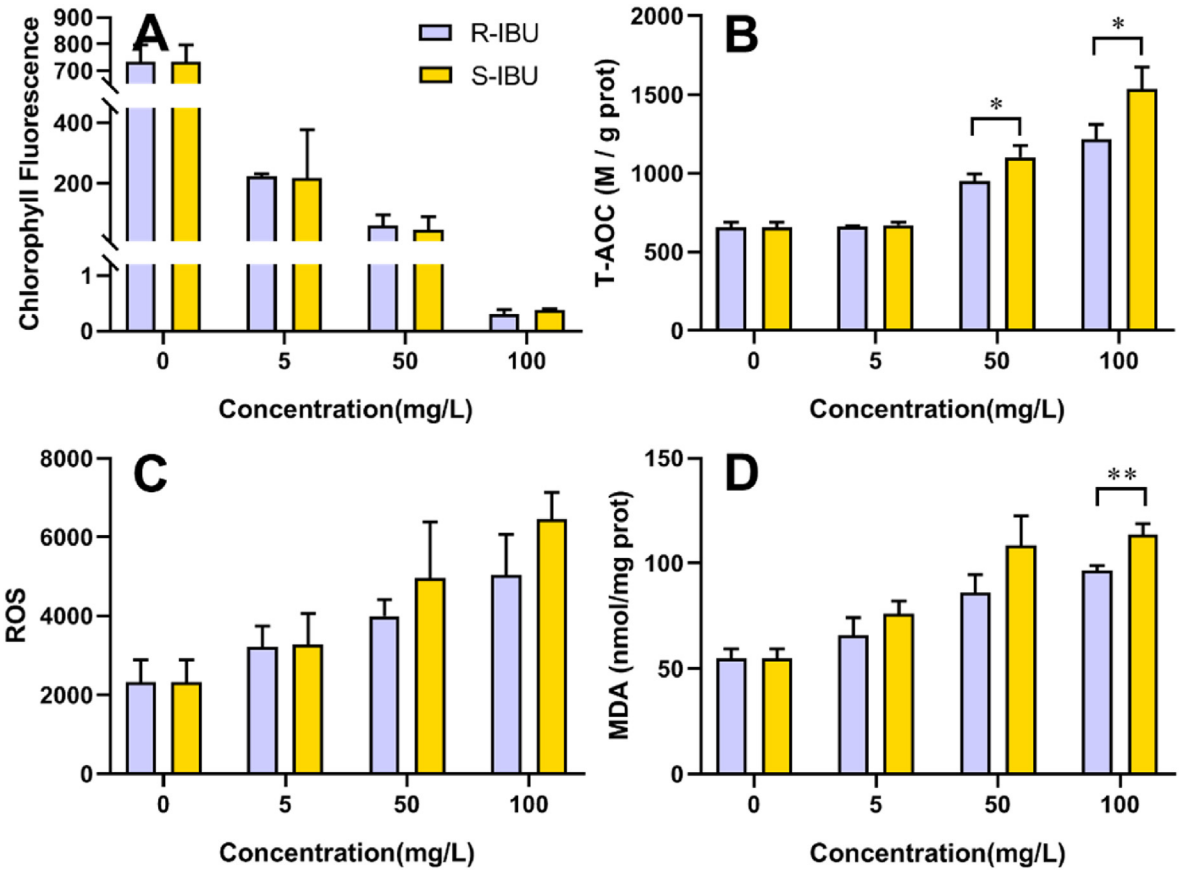

Fig. 2. The influences on (A) chlorophyll fluorescence, (B) T-AOC, (C) ROS and (D) MDA of *C. pyrenoidosa* exposed by R- and S-IBU in the absence of 1 mg L^{-1} NP. The results are the means from three independent replicates; the error bars correspond to the standard deviation; one and two asterisks denote significant differences between the R-IBU and S-IBU exposure groups at $p < 0.05$ and $p < 0.01$, respectively (LSD Test).

value was 25.8% when NP were present, showing that 1 mg L^{-1} NP had no significant effect on the abiotic degradation of IBU.

Fig. 6A shows the concentrations-time curves of rac-IBU in the algae medium. In the treatment without NP, approximately 28.6% of rac-IBU had degraded at the end of the experiment and the corresponding value in the treatment containing NP was 29.7%, suggesting that NP slightly accelerated the removal of rac-IBU in the algae medium. As shown in Fig. 5B, the EF values of IBU in the medium were below 0.5 during the experiment, indicating the preferential removal of R-IBU, which may be due to the preferential accumulation and degradation of R-IBU in the algae.

After 42 days, approximately 30.8% and 29.2% of R- and S-IBU, respectively, degraded in the NP-free medium, and the corresponding values in the NP treatments were 32.1% and 30.5%, respectively, indicating the preferential removal of R-IBU in both the absence and presence of NP. These results implied that the co-presence of 1 mg L^{-1} NP had no effect on the enantioselective removal of IBU in the medium.

4. Discussion

The widespread microplastic pollution in freshwaters has aroused considerable public concern (Mani et al., 2015; Zhang et al., 2015a). As an vital primary producter in aquatic ecosystem, algae can potentially alter ecosystem functions. Previous researches have found that microplastics could inhibit the growth rate of algae, which closely depend on their size and dose instead of the polymer composition (Lei et al., 2018; Sjollema et al., 2016). Large microplastics in the ppm range have no significant influences on the growth rate of algae. For instance, no apparent changes in the growth rate of *Skeletonema costatum* were observed after exposure to polyvinyl chloride (PVC, 1 mm) at 50 mg L^{-1} (Zhang et al., 2017). Polypropylene (PP) and high-density polyethylene (HDPE) (400–1000 μm) at 1000 mg L^{-1} did not affect the growth rate of *Chlamydomonas reinhardtii* (Lagarde et al., 2016). However, smaller-sized microplastics could exhibit inhibition effects on algae growth (Lei et al., 2018; Sjollema et al., 2016). Exposure to 25 mg L^{-1} PS (6 μm) caused a small inhibition (<10%) in the growth rate of *Dunaliella tertiolecta* (Sjollema et al., 2016). The growth of *C. pyrenoidosa* was inhibited by 20.9% after exposure to PS (1 μm) at 10 mg L^{-1} (Mao et al., 2018). The growth rates of the diatom *Thalassiosira weissflogii* were significantly reduced after exposure to polymethyl methacrylate (PMMA, 40 nm) at 18.8 mg L^{-1} (Venâncio et al., 2019). In this study, PS (0.6 μm) at 1 mg L^{-1} inhibited the growth of *C. pyrenoidosa* by 15.6% after 4 days of exposure, indicating that more attention should be paid to the toxicity of NP. As a matter of fact, nanoparticles may exert negative effects on algae, such as direct toxic effects and indirect physical shading effect (Sørensen et al., 2016; Schwab et al., 2011). In this work, due to the low NP concentration and non-aggregation, NP shading only contributed to 1.21 ± 1.76% of the growth inhibition. This indicated that 1 mg L^{-1} PS NP inhibited algae growth by a direct toxic effect, which may mainly be due to the adsorption of NP on the cell wall of algae and the entrance of NP into the algae cell (Nolte et al., 2017).

Considering the co-existence of microplastics and PPCPs in the aquatic environment, their combined effects is a matter of concern.

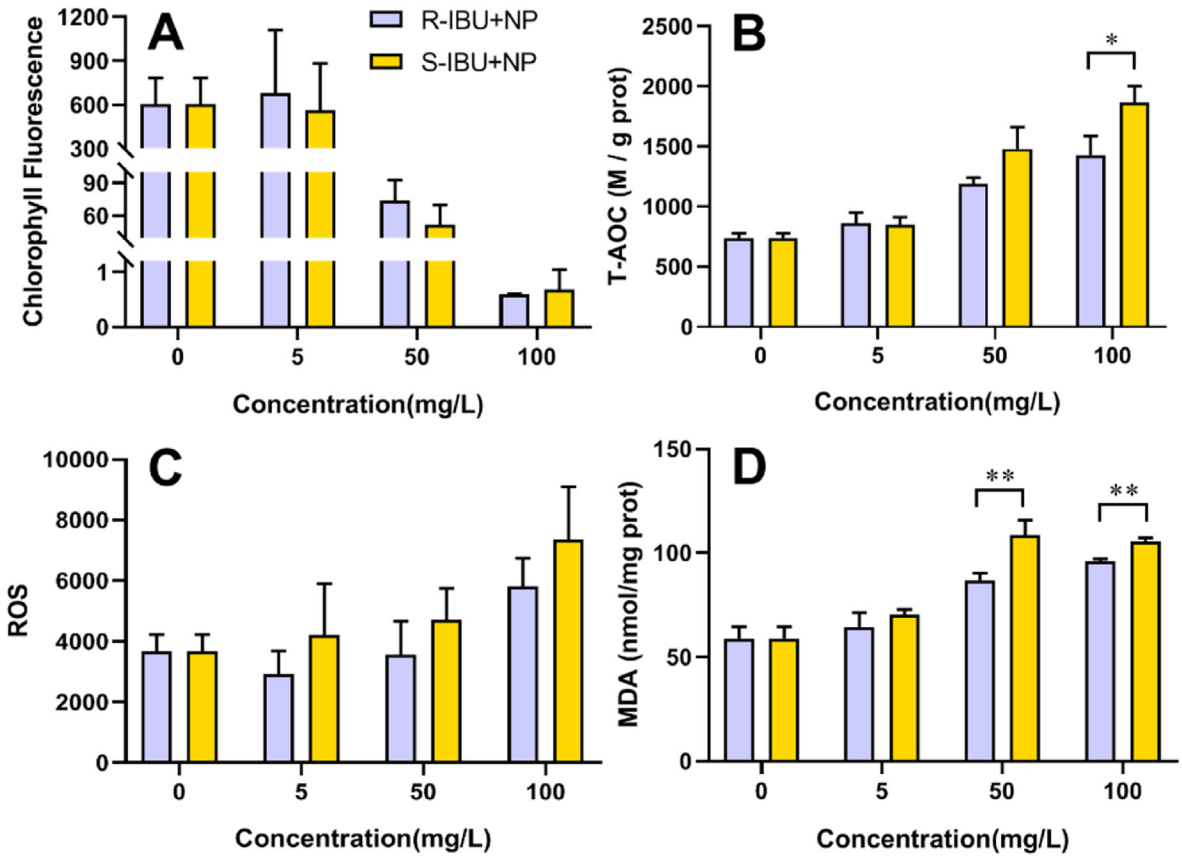

Fig. 3. The influences on (A) chlorophyll fluorescence, (B) T-AOC, (C) ROS and (D) MDA of *C. pyrenoidosa* exposed by R- and S-IBU in the presence of 1 mg L^{-1} NP. The results are the means from three independent replicates; the error bars correspond to the standard deviation; one and two asterisks denote significant differences between the R-IBU + NP and S-IBU + NP exposure groups at $p < 0.05$ and $p < 0.01$, respectively (LSD Test).

This study investigated the acute toxicity of IBU on *C. pyrenoidosa* growth in the absence and presence of NP, and found NP could mitigate the inhibitory effect of IBU on algae growth. This was similar to the results of previous reports (Davarpanah and Guilhermino, 2015; Yang et al., 2020; Zhang et al., 2018; Zhu et al., 2019). Polyethylene (PE) microplastics could decrease the Cu-induced growth inhibition in *Tetraselmis chuii* (Davarpanah and Guilhermino, 2015). The inhibitory effect of glyphosate on *Microcystis aeruginosa* was alleviated when PS-NH_2 microplastics were present (Zhang et al., 2018). Microplastics had positive effect in terms of alleviating nonylphenol toxicity to *C. pyrenoidosa* (Yang et al., 2020). The presence of microplastics decreased the toxicity of triclosan on *Skeletonema costatum* (Zhu et al., 2019). Organisms possess antioxidant defense systems that can protect against lipid peroxidation by efficiently scavenging ROS. The T-AOC represents the overall antioxidative capability, including the capacity of enzymatic and non-enzymatic antioxidants. Lipid peroxidation was generally determined by its secondary product (MDA). In the current study, the co-exposure of NP led to a significant enhancement of the T-AOC, a slight reduction of the ROS, MDA and IBU accumulation in *C. pyrenoidosa* compared with the individual exposure (IBU) group. This was possibly due to the adsorption of IBU on NP, thereby making them less bioavailable and mitigating the inhibitory effect of IBU on *C. pyrenoidosa* growth (Chua et al., 2014; Davarpanah and Guilhermino, 2015; Sørensen et al., 2020). Similarly, the toxicity and bioavailability of Cu in *Tetraselmis chuii* decreased in the presence of PE microplastics (Davarpanah and Guilhermino, 2015).

Currently, some studies have investigated the influence of microplastics on the toxicity of other pollutants; however, the effects of microplastics on the biodegradation of pollutants in aquatic organisms were poorly documented. In this study, the degradation of IBU in *C. pyrenoidosa* was promoted by the presence of NP, which was possibly caused by the enhancement of the metabolic enzyme activity in *C. pyrenoidosa*. It has been reported that the metabolic enzyme activity was elevated in the presence of cadmium, thereby enhancing the degradation of permethrin in *Chironomus dilutus* (Chen et al., 2016). The co-exposure of ketoconazole inhibited the metabolic enzymatic activity, resulting in a decreased metabolism of BPA in *Danio rerio* (Ji et al., 2019). The combined exposure of PS and carbamazepine led to an activation in carbamazepine biotransformation phase I reactions in *Mytilus galloprovincialis* (Brandts et al., 2018). Besides, NP slightly accelerated the removal of rac-IBU in the algae mediumm, which maybe because the presence of NP decreased the toxicity and accelerated the degradation of rac-IBU in the algae.

Enantiomers of chiral compounds may exhibit different toxicities, accumulation and degradation behaviors in algae. For instance, R-benalaxyl showed higher toxicity and S-benalaxyl was preferentially degraded in *Scenedesmus obliquus* (Huang et al., 2012). The toxicity, uptake and digestion of cyproconazole to *C. pyrenoidosa* were enantioselective (Zhang et al., 2016b). In this study, enantioselective toxicity, accumulation and degradation of IBU in *C. pyrenoidosa* were observed, with S-IBU being more toxic and R-IBU being preferentially accumulated and degraded. Though the co-exposure of NP led to a decreased toxicity, bioaccumulation and an increased biodegradation of IBU in *C. pyrenoidosa*, the enantioselective toxic effects, accumulation and degradation of IBU

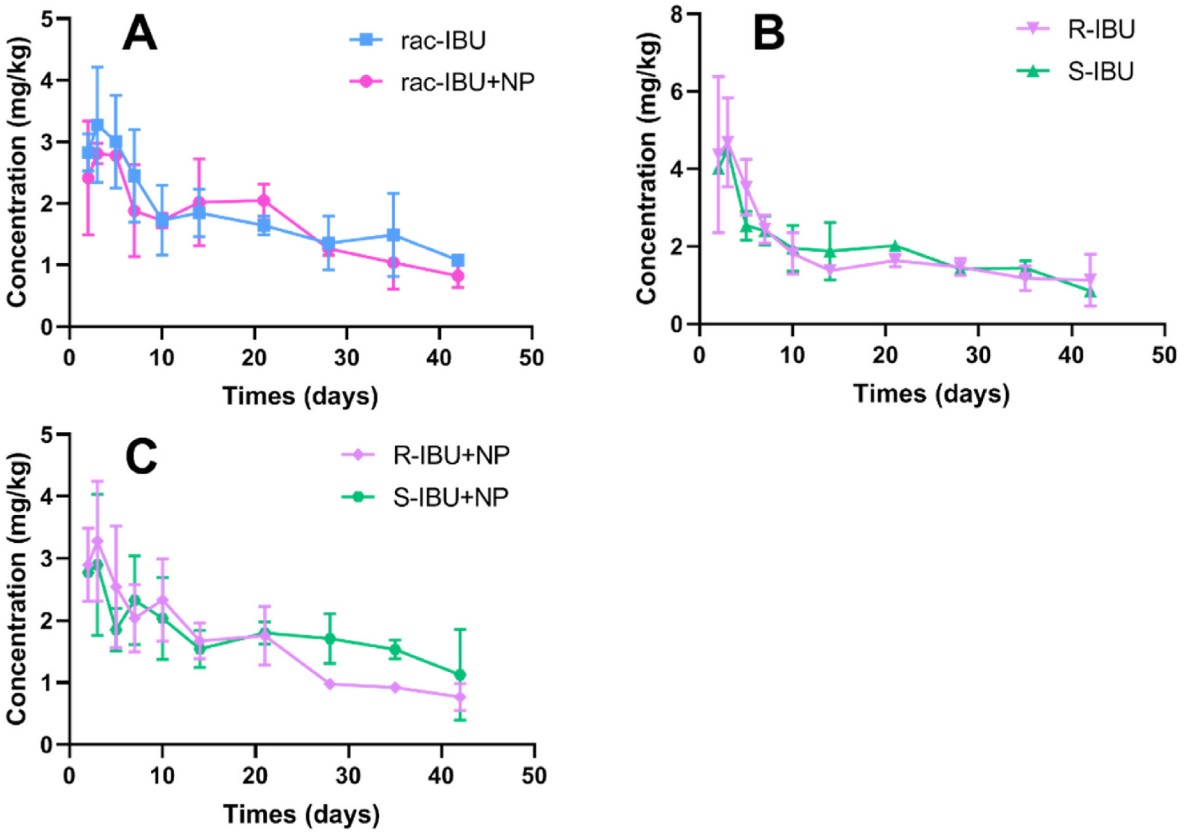

Fig. 4. Concentrations-time curves of IBU in *C. pyrenoidosa* exposed to (A) 0.5 mg L^{-1} rac-IBU in the absence and presence of 1 mg L^{-1} NP, (B) 0.5 mg L^{-1} R- and S-IBU in the absence of NP, (C) 0.5 mg L^{-1} R- and S-IBU in the presence of 1 mg L^{-1} NP. The results are the means from three independent replicates; the error bars correspond to the standard deviation.

Table 2
The degradation parameters of IBU in *C. pyrenoidosa*.

Compounds	Control group			NP group		
	Regression equation[a]	R^2 [b]	$T_{1/2}$ (d)	Regression equation[a]	R^2 [b]	$T_{1/2}$ (d)
rac-IBU	$y = 2.90e^{-0.024x}$	0.822	28.9	$y = 2.83e^{-0.028x}$	0.867	24.8
R-IBU	$y = 3.52e^{-0.031x}$	0.753	22.4	$y = 3.08e^{-0.035x}$	0.914	19.8
S-IBU	$y = 3.30e^{-0.029x}$	0.804	23.9	$y = 2.80e^{-0.030x}$	0.770	23.1

[a] The regression equations are constructed based on the mean values of three replicates.
[b] R^2 corresponds to correlation coefficient.

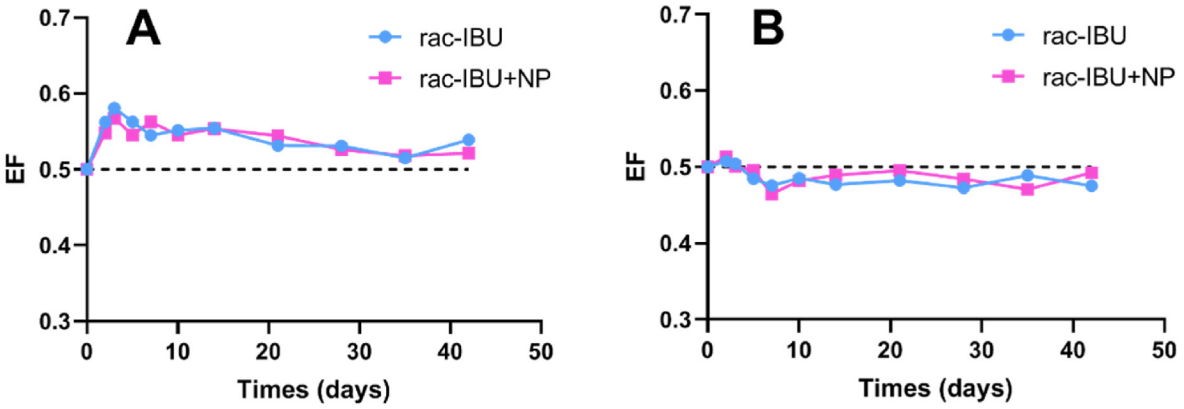

Fig. 5. EF values of IBU in (A) *C. pyrenoidosa* and (B) growth medium after racemic IBU exposure.

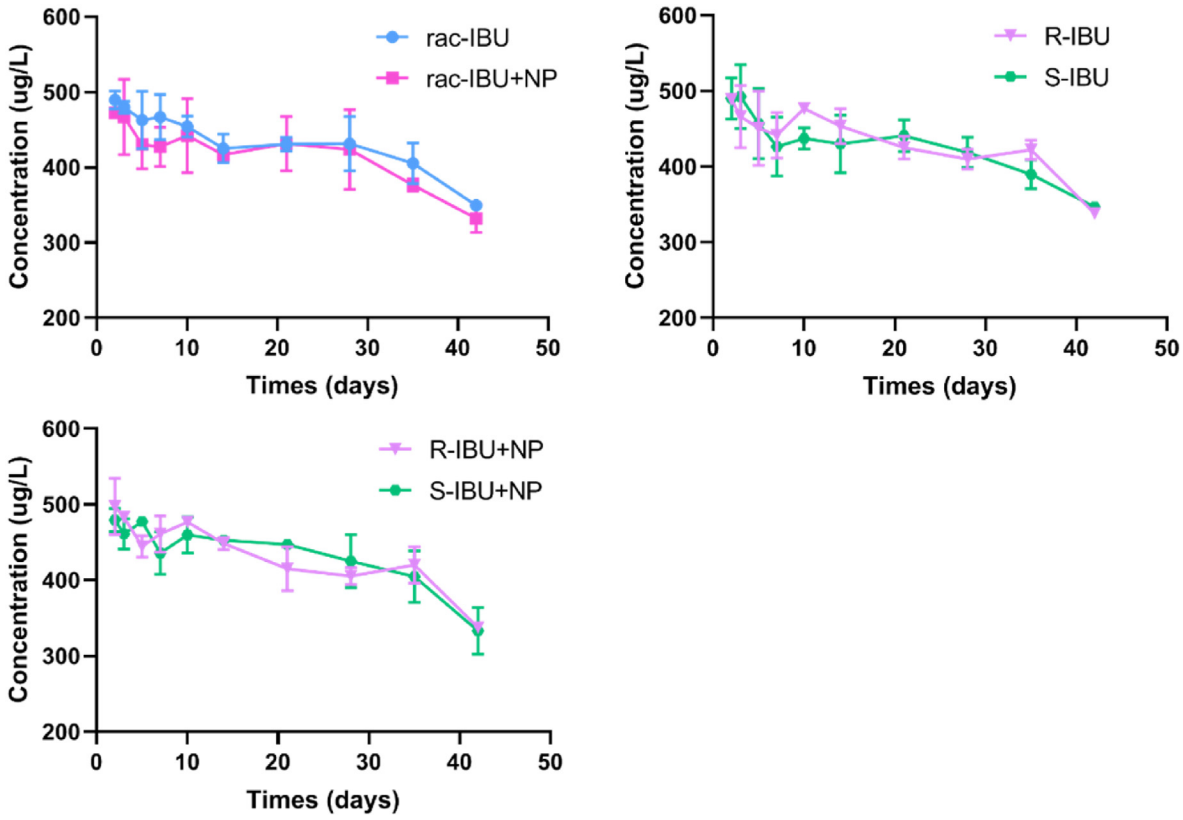

Fig. 6. Concentrations-time curves of IBU in the medium exposed to (A) 0.5 mg L^{-1} rac-IBU in the presence and absence of 1 mg L^{-1} NP, (B) 0.5 mg L^{-1} R- and S-IBU in the absence of MP, (C) 0.5 mg L^{-1} R- and S-IBU in the presence of 1 mg L^{-1} NP. The results are the means from three independent replicates; the error bars correspond to the standard deviation.

still existed when NP were present. Few research have investigated the effect of micro- or nanoplastics on the enantioselectivity of pollutants in algae. Our results was in accordance with those reported for other organisms (Li et al., 2019; Qu et al., 2019). For instance, the impacts of venlafaxine on the SOD and MDA in *Misgurnus anguillicaudatus* were enantioselective in both individual (venlafaxine) and the co-exposure (venlafaxine + PVC) groups (Qu et al., 2019). The preferential enrichment of (-) α-, β-, and γ-HBCD in *Eisenia fetida* was observed in the absence and presence of PS microplastics (Li et al., 2019). However, the influence of co-existent pollutants on chiral conversion is still unknown. Ibuprofen was chosen in this study partially due to the interconversion between the enantiomers. For instance, S-IBU could transform into R-IBU during wastewater treatment processes, and R-IBU could convert into S-IBU during human metabolism (Hao et al., 2005; Matamoros et al., 2009). However, no interconversion of the two enantiomers in *C. pyrenoidosa* was observed regardless of the presence of NP. Thus, the influence of NP on chiral conversion needs further investigation.

5. Conclusion

The extensive existence of microplastics in the environment has received a substantial amount of attention. NP may pose greater risks to organisms than its microsized counterparts due to its easier uptake. The effects of NP on the toxic effects, bioaccumulation, biodegradation and enantioselectivity of IBU in *C. pyrenoidosa* were reported in this study. The growth inhibitory effect and oxidative stress induced by IBU was reduced in the presence of NP. In addition, the co-presence of NP decreased the accumulation level, accelerated the degradation of IBU in *C. pyrenoidosa* and enhanced removal in the medium. NP had no significant effect on the enantioselectivity of IBU, which occurred in both the absence and presence of NP. S-IBU was more toxic, and R-IBU was preferentially accumulated and degraded in *C. pyrenoidosa*. No interconversion of the two enantiomers occurred regardless of the presence of NP. The findings of this work provide a basis for the comprehensive assessment of NP environmental risks.

Declaration of competing interest

The authors declare that they have no known competing financial interests or personal relationships that could have appeared to influence the work reported in this paper.

CRediT authorship contribution statement

Fang Wang: Conceptualization, Methodology, Writing - original draft. **Bin Wang:** Project administration, Funding acquisition, Writing - review & editing. **Han Qu:** Investigation, Validation. **Wenxing Zhao:** Formal analysis. **Lei Duan:** Data curation, Software. **Yizhe Zhang:** Resources. **Yitong Zhou:** Visualization. **Gang Yu:** Supervision.

Acknowledgements

This work was supported by the Major Science and Technology Program for Water Pollution Control and Treatment in China, China (Contract Grants 2017ZX07202006) and the National Natural Science Foundation of China, China (Contract Grants 21577075)..

Appendix A. Supplementary data

Supplementary data to this article can be found online at https://doi.org/10.1016/j.envpol.2020.114593.

References

Bagnall, J., Malia, L., Lubben, A., Kasprzyk-Hordern, B., 2013. Stereoselective biodegradation of amphetamine and methamphetamine in river microcosms. Water Res. 47, 5708–5718.

Baird, S., Garrison, A., Jones, J., Avants, J., Bringolf, R., Black, M., 2013. Enantioselective toxicity and bioaccumulation of fipronil in fathead minnows (Pimephales promelas) following water and sediment exposures. Environ. Toxicol. Chem. 32, 222–227.

Bradford, M.M., 1976. A rapid and sensitive method for the quantitation of microgram quantities of protein utilizing the principle of protein-dye binding. Anal. Biochem. 72, 248–254.

Brandts, I., Teles, M., Gonçalves, A.P., Barreto, A., Franco-Martinez, L., Tvarijonaviciute, A., Martins, M.A., Soares, A.M.V.M., Tort, L., Oliveira, M., 2018. Effects of nanoplastics on Mytilus galloprovincialis after individual and combined exposure with carbamazepine. Sci. Total Environ. 643, 775–784.

Bu, Q., Wang, B., Huang, J., Deng, S., Yu, G., 2013. Pharmaceuticals and personal care products in the aquatic environment in China: a review. J. Hazard Mater. 262, 189–211.

Buser, H.-R., Poiger, T., Müller, M.D., 1999. Occurrence and environmental behavior of the chiral pharmaceutical drug ibuprofen in surface waters and in wastewater. Environ. Sci. Technol. 33, 2529–2535.

Chen, X., Li, H., Zhang, J., Ding, Y., You, J., 2016. Does cadmium affect the toxicokinetics of permethrin in Chironomus dilutus at sublethal level? Evidence of enzymatic activity and gene expression. Environ. Pollut. 218, 1005–1013.

Chua, E.M., Shimeta, J., Nugegoda, D., Morrison, P.D., Clarke, B.O., 2014. Assimilation of polybrominated diphenyl ethers from microplastics by the marine amphipod, allorchestes compressa. Environ. Sci. Technol. 48, 8127–8134.

Davarpanah, E., Guilhermino, L., 2015. Single and combined effects of microplastics and copper on the population growth of the marine microalgae Tetraselmis chuii. Estuar. Coast Shelf Sci. 167, 269–275.

Eriksen, M., Lebreton, L.C.M., Carson, H.S., Thiel, M., Moore, C.J., Borerro, J.C., Galgani, F., Ryan, P.G., Reisser, J., 2014. Plastic pollution in the world's oceans: more than 5 trillion plastic pieces weighing over 250,000 tons afloat at sea. PloS One 9, e111913.

Escuder-Gilabert, L., Martín-Biosca, Y., Perez-Baeza, M., Sagrado, S., Medina-Hernández, M.J., 2018. Direct chromatographic study of the enantioselective biodegradation of ibuprofen and ketoprofen by an activated sludge. J. Chromatogr. A 1568, 140–148.

Evans, S.E., Bagnall, J., Kasprzyk-Hordern, B., 2016. Enantioselective degradation of amphetamine-like environmental micropollutants (amphetamine, methamphetamine, MDMA and MDA) in urban water. Environ. Pollut. 215, 154–163.

Gao, J., Wang, F., Wang, P., Jiang, W., Zhang, Z., Liu, D., Zhou, Z., 2019. Enantioselective toxic effects and environmental behavior of ethiprole and its metabolites against Chlorella pyrenoidosa. Environ. Pollut. 244, 757–765.

Hao, H., Wang, G., Sun, J., 2005. Enantioselective pharmacokinetics of ibuprofen and involved mechanisms. Drug Metabol. Rev. 37, 215–234.

Heath, R.L., Packer, L., 1968. Photoperoxidation in isolated chloroplasts: I. Kinetics and stoichiometry of fatty acid peroxidation. Arch. Biochem. Biophys. 125, 189–198.

Huang, L., Lu, D., Diao, J., Zhou, Z., 2012. Enantioselective toxic effects and biodegradation of benalaxyl in Scenedesmus obliquus. Chemosphere 87, 7–11.

Jambeck, J.R., Geyer, R., Wilcox, C., Siegler, T.R., Perryman, M., Andrady, A., Narayan, R., Law, K.L., 2015. Plastic waste inputs from land into the ocean. Science 347, 768–771.

Ji, K., Seo, J., Kho, Y., Choi, K., 2019. Co-exposure to ketoconazole alters effects of bisphenol A in Danio rerio and H295R cells. Chemosphere 237, 124414.

Kasprzyk-Hordern, B., Dinsdale, R.M., Guwy, A.J., 2009. The removal of pharmaceuticals, personal care products, endocrine disruptors and illicit drugs during wastewater treatment and its impact on the quality of receiving waters. Water Res. 43, 363–380.

Kasprzyk-Hordern, B., Kondakal, V.V.R., Baker, D.R., 2010. Enantiomeric analysis of drugs of abuse in wastewater by chiral liquid chromatography coupled with tandem mass spectrometry. J. Chromatogr. A 1217, 4575–4586.

Khan, S.J., Wang, L., Hashim, N.H., Mcdonald, J.A., 2014. Distinct enantiomeric signals of ibuprofen and naproxen in treated wastewater and sewer overflow. Chirality 26, 739–746.

Lagarde, F., Olivier, O., Zanella, M., Daniel, P., Hiard, S., Caruso, A., 2016. Microplastic interactions with freshwater microalgae: hetero-aggregation and changes in plastic density appear strongly dependent on polymer type. Environ. Pollut. 215, 331–339.

Lambert, S., Wagner, M., 2016. Characterisation of nanoplastics during the degradation of polystyrene. Chemosphere 145, 265–268.

Lei, L., Wu, S., Lu, S., Liu, M., Song, Y., Fu, Z., Shi, H., Raley-Susman, K.M., He, D., 2018. Microplastic particles cause intestinal damage and other adverse effects in zebrafish Danio rerio and nematode Caenorhabditis elegans. Sci. Total Environ. 619–620, 1–8.

Li, B., Lan, Z., Wang, L., Sun, H., Yao, Y., Zhang, K., Zhu, L., 2019. The release and earthworm bioaccumulation of endogenous hexabromocyclododecanes (HBCDDs) from expanded polystyrene foam microparticles. Environ. Pollut. 255, 113163.

Loraine, G.A., Pettigrove, M.E., 2006. Seasonal variations in concentrations of pharmaceuticals and personal care products in drinking water and reclaimed wastewater in southern California. Environ. Sci. Technol. 40, 687–695.

Mani, T., Hauk, A., Walter, U., Burkhardt-Holm, P., 2015. Microplastics profile along the Rhine River. Sci. Rep. 5, 17988.

Mao, Y., Ai, H., Chen, Y., Zhang, Z., Zeng, P., Kang, L., Li, W., Gu, W., He, Q., Li, H., 2018. Phytoplankton response to polystyrene microplastics: perspective from an entire growth period. Chemosphere 208, 59–68.

Matamoros, V., Hijosa, M., Bayona, J.M., 2009. Assessment of the pharmaceutical active compounds removal in wastewater treatment systems at enantiomeric level. Ibuprofen and naproxen. Chemosphere 75, 200–205.

Nolte, T.M., Hartmann, N.B., Kleijn, J.M., Garnæs, J., van de Meent, D., Jan Hendriks, A., Baun, A., 2017. The toxicity of plastic nanoparticles to green algae as influenced by surface modification, medium hardness and cellular adsorption. Aquat. Toxicol. 183, 11–20.

OECD, 2011. Test No. 201: Freshwater Alga and Cyanobacteria. Growth Inhibition Test.

Peng, F.-Q., Ying, G.-G., Yang, B., Liu, S., Lai, H.-J., Liu, Y.-S., Chen, Z.-F., Zhou, G.-J., 2014. Biotransformation of progesterone and norgestrel by two freshwater microalgae (Scenedesmus obliquus and Chlorella pyrenoidosa): transformation kinetics and products identification. Chemosphere 95, 581–588.

Peng, X., Yu, Y., Tang, C., Tan, J., Huang, Q., Wang, Z., 2008. Occurrence of steroid estrogens, endocrine-disrupting phenols, and acid pharmaceutical residues in urban riverine water of the Pearl River Delta, South China. Sci. Total Environ. 397, 158–166.

Qu, H., Ma, R., Wang, B., Yang, J., Duan, L., Yu, G., 2019. Enantiospecific toxicity, distribution and bioaccumulation of chiral antidepressant venlafaxine and its metabolite in loach (Misgurnus anguillicaudatus) co-exposed to microplastic and the drugs. J. Hazard Mater. 370, 203–211.

Re, R., Pellegrini, N., Proteggente, A., Pannala, A., Yang, M., Rice-Evans, C., 1999. Antioxidant activity applying an improved ABTS radical cation decolorization assay. Free Radic. Biol. Med. 26, 1231–1237.

Sørensen, L., Rogers, E., Altin, D., Salaberria, I., Booth, A.M., 2020. Sorption of PAHs to microplastic and their bioavailability and toxicity to marine copepods under co-exposure conditions. Environ. Pollut. 258, 113844.

Sørensen, S.N., Engelbrekt, C., Lützhøft, H.-C.H., Jiménez-Lamana, J., Noori, J.S., Alatraktchi, F.A., Delgado, C.G., Slaveykova, V.I., Baun, A., 2016. A multimethod approach for investigating algal toxicity of platinum nanoparticles. Environ. Sci. Technol. 50, 10635–10643.

Santos, J.L., Aparicio, I., Alonso, E., 2007. Occurrence and risk assessment of pharmaceutically active compounds in wastewater treatment plants. A case study: seville city (Spain). Environ. Int. 33, 596–601.

Schwab, F., Bucheli, T.D., Lukhele, L.P., Magrez, A., Nowack, B., Sigg, L., Knauer, K., 2011. Are carbon nanotube effects on green algae caused by shading and agglomeration? Environ. Sci. Technol. 45, 6136–6144.

Sjollema, S.B., Redondo-Hasselerharm, P., Leslie, H.A., Kraak, M.H.S., Vethaak, A.D., 2016. Do plastic particles affect microalgal photosynthesis and growth? Aquat. Toxicol. 170, 259–261.

Song, Y., Chai, T., Yin, Z., Zhang, X., Zhang, W., Qian, Y., Qiu, J., 2018. Stereoselective effects of ibuprofen in adult zebrafish (Danio rerio) using UPLC-TOF/MS-based metabolomics. Environ. Pollut. 241, 730–739.

Stanley, J.K., Ramirez, A.J., Chambliss, C.K., Brooks, B.W., 2007. Enantiospecific sublethal effects of the antidepressant fluoxetine to a model aquatic vertebrate and invertebrate. Chemosphere 69, 9–16.

Steiner, T., Ahmed, F., Findley, L., MacGregor, E., Wilkinson, M., 1998. S-fluoxetine in the prophylaxis of migraine: a phase II double-blind randomized placebo-controlled study. Cephalalgia 18, 283–286.

Sussarellu, R., Suquet, M., Thomas, Y., Lambert, C., Fabioux, C., Pernet, M.E.J., Le Goïc, N., Quillien, V., Mingant, C., Epelboin, Y., Corporeau, C., Guyomarch, J., Robbens, J., Paul-Pont, I., Soudant, P., Huvet, A., 2016. Oyster reproduction is affected by exposure to polystyrene microplastics. Proc. Natl. Acad. Sci. Unit. States Am. 113, 2430–2435.

Thompson, R.C., Olsen, Y., Mitchell, R.P., Davis, A., Rowland, S.J., John, A.W.G., McGonigle, D., Russell, A.E., 2004. Lost at sea: where is all the plastic? Science 304, 838-838.

Venàncio, C., Ferreira, I., Martins, M.A., Soares, A.M.V.M., Lopes, I., Oliveira, M., 2019. The effects of nanoplastics on marine plankton: a case study with polymethylmethacrylate. Ecotoxicol. Environ. Saf. 184, 109632.

Wang, S., Poon, K., Cai, Z., 2018. Removal and metabolism of triclosan by three different microalgal species in aquatic environment. J. Hazard Mater. 342, 643–650.

Winkler, M., Lawrence, J.R., Neu, T.R., 2001. Selective degradation of ibuprofen and clofibric acid in two model river biofilm systems. Water Res. 35, 3197–3205.

Xia, B., Sui, Q., Sun, X., Han, Q., Chen, B., Zhu, L., Qu, K., 2018. Ocean acidification increases the toxic effects of TiO2 nanoparticles on the marine microalga Chlorella vulgaris. J. Hazard Mater. 346, 1–9.

Yang, W., Gao, X., Wu, Y., Wan, L., Tan, L., Yuan, S., Ding, H., Zhang, W., 2020. The combined toxicity influence of microplastics and nonylphenol on microalgae Chlorella pyrenoidosa. Ecotoxicol. Environ. Saf. 195, 110484.

Ye, J., Wang, L., Zhang, Z., Liu, W., 2013. Enantioselective physiological effects of the herbicide diclofop on cyanobacterium Microcystis aeruginosa. Environ. Sci. Technol. 47, 3893–3901.

Zhang, C., Chen, X., Wang, J., Tan, L., 2017. Toxic effects of microplastic on marine microalgae Skeletonema costatum: interactions between microplastic and algae. Environ. Pollut. 220, 1282–1288.
Zhang, K., Gong, W., Lv, J., Xiong, X., Wu, C., 2015a. Accumulation of floating microplastics behind the three gorges dam. Environ. Pollut. 204, 117–123.
Zhang, Q., Hua, X.-d., Shi, H.-y., Liu, J.-s., Tian, M.-m., Wang, M.-h., 2015b. Enantioselective bioactivity, acute toxicity and dissipation in vegetables of the chiral triazole fungicide flutriafol. J. Hazard Mater. 284, 65–72.
Zhang, Q., Qu, Q., Lu, T., Ke, M., Zhu, Y., Zhang, M., Zhang, Z., Du, B., Pan, X., Sun, L., Qian, H., 2018. The combined toxicity effect of nanoplastics and glyphosate on Microcystis aeruginosa growth. Environ. Pollut. 243, 1106–1112.
Zhang, S., Lin, D., Wu, F., 2016a. The effect of natural organic matter on bioaccumulation and toxicity of chlorobenzenes to green algae. J. Hazard Mater. 311, 186–193.
Zhang, W., Cheng, C., Chen, L., Di, S., Liu, C., Diao, J., Zhou, Z., 2016b. Enantioselective toxic effects of cyproconazole enantiomers against Chlorella pyrenoidosa. Chemosphere 159, 50–57.
Zhao, J., Cao, X., Wang, Z., Dai, Y., Xing, B., 2017. Mechanistic understanding toward the toxicity of graphene-family materials to freshwater algae. Water Res. 111, 18–27.
Zhu, Z.-l., Wang, S.-c., Zhao, F.-f., Wang, S.-g., Liu, F.-f., Liu, G.-z., 2019. Joint toxicity of microplastics with triclosan to marine microalgae Skeletonema costatum. Environ. Pollut. 246, 509–517.